



Estimation of vegetative mercury emissions in China

QUAN Jiannong¹, ZHANG Xiaoshan^{1,*}, Shang Gyoo SHIM²

1. Research Center for Eco-Environmental Sciences, Chinese Academy of Sciences, Beijing 100085, China.

E-mail: quanjn1975@gmail.com

2. Korea Institute of Science and Technology, Seoul 136-791, Korea

Received 11 September 2007; revised 18 October 2007; accepted 5 November 2007

Abstract

Vegetative mercury emissions were estimated within the framework of Biogenic Emission Inventory System (BEIS3 V3.11). In this estimation, the 19 categories of U.S. Geological Survey landcover data were incorporated to generate the vegetation-specific mercury emissions in a 81-km Lambert Conformal model grid covering the total Chinese continent. The surface temperature and cloud-corrected solar radiation from a Mesoscale Meteorological model (MM5) were retrieved and used for calculating the diurnal variation. The implemented emission factors were either evaluated from the measured mercury flux data for forest, agriculture and water, or assumed for other land fields without available flux data. Annual simulations using the MM5 data were performed to investigate the seasonal emission variation. From the sensitivity analysis using two sets of emission factors, the vegetative mercury emissions in China domain were estimated to range from a lower limit of 79×10^3 kg/year to an upper limit of 177×10^3 kg/year. The modeled vegetative emissions were mainly generated from the eastern and southern China. Using the estimated data, it is shown that mercury emissions from vegetation are comparable to that from anthropogenic sources during summer. However, the vegetative emissions decrease greatly during winter, leaving anthropogenic sources as the major sources of emission.

Key words: mercury emission; Biogenic Emission Inventory System (BEIS3); natural source

Introduction

Terrestrial surfaces are unequivocally important in mercury (Hg) cycling between the atmosphere and the Earth's surface (Lindberg, 1996). Hg can be emitted from terrestrial surfaces to the atmosphere and deposited to terrestrial surfaces from the atmosphere by wet and dry processes. Hg emissions from anthropogenic sources have increased Hg deposition, which could significantly alter the basic picture of natural Hg cycling (Kim *et al.*, 1997). Field measurements of Hg air/soil surface exchange have been increasing in this decade, and the results show the essential roles of soils in the regional and global cycling of Hg (Kim *et al.*, 1997; Carpi and Lindberg, 1998; Zhang and Lindberg, 1999; Feng *et al.*, 2005). Soils enriched with Hg have been considered to be important sources contributing to the atmospheric Hg load (Rasmussen, 1994; Gustin *et al.*, 2003). The latest field investigations indicated that these natural sources may be comparable to the anthropogenic sources in their impacts on regional and global atmospheric Hg pools (Gustin *et al.*, 1999).

The Hg emissions in China continue at high levels because of the large quantities of coal combustion and the extent of other mercury-releasing activities. The estimated anthropogenic Hg emissions in China were 536×10^3 kg

in 2000 (Streets *et al.*, 2005). Pacyna and Pacyna (2002) estimated that Hg emissions from China contributed more than 25% to total global emissions. High Hg emissions lead to high Hg concentration in air (Liu *et al.*, 2002; Feng *et al.*, 2003) and high Hg deposition in some areas of China (Fang *et al.*, 2001; Xiao *et al.*, 1998; Tan *et al.*, 2000; Feng *et al.*, 2002). Hg content in soil has also increased accordingly, especially in and around cities and industrial areas (Hou *et al.*, 2005a; Wang *et al.*, 2005; Fang and Wang, 2004; Lin *et al.*, 2007; Lai *et al.*, 2005). All of the above works are important to understand the situation of Hg contamination in China. But, till date there is no report on total vegetative Hg emissions in China except for some regional estimation (Feng *et al.*, 2005; Zhang *et al.*, 2005; Wang *et al.*, 2005). Therefore, it is necessary to estimate total Hg emission from vegetative sources in China to understand its roles in Hg cycling.

In this article, vegetative Hg emissions in the total Chinese continent domain within the framework of Biogenic Emission Inventory System Version 3.11 (BEIS3; Lamb *et al.*, 1993) was estimated. BEIS3 calculates the temporally and spatially resolved vegetative emissions of Hg based on landuse/landcover data, meteorological fields, and Hg emission flux ($\text{ng}/(\text{m}^2 \cdot \text{h})$) for given landuse type or vegetation species.

* Corresponding author. E-mail: zhangxsh@rcees.ac.cn.

1 Method

1.1 Models, domain and input data

The version 3.11 of BEIS3 was used in this article, a stand-alone research version on UNIX/Linux platform. The model calculates the plant-species-specific emissions of volatile organic compounds (VOCs) and NO_x for the landuse/landcover types listed in the U.S. Geological Survey Biogenic Emissions Landcover Data Version 3 (BELD3) datasets. The BELD3 data, along with the Hg emission factors estimated from this work, were used to generate the normalized vegetation-specific Hg emissions in a 81-km Lambert Conformal grid covering the entire Chinese continent (Fig.1). The surface temperature and cloud-cover-corrected solar radiation from a Mesoscale Meteorological model (MM5 Version 3.6, Grell *et al.*, 1994) were retrieved and converted into model-ready format using a Meteorological Chemistry Interface Processor (MCIP2, Byun and Ching, 1999). The converted data were used for temperature and solar radiation corrections to calculate the diurnal variation of vegetative emissions. To estimate the annual mercury emissions from vegetation

and its seasonal variation, the hourly meteorological fields of 2003 in an annual simulation was used.

1.2 Model implementation

A regression-based model was used to estimate the Hg emission flux from vegetation. The goal of the regression-based approach was to assimilate the modeled Hg emission intensity to the field observation of Hg flux. The diurnal variation of the modeled Hg flux was simulated through the correction factors of solar irradiation and temperature at earth's surface, i.e:

$$F_i = F_{s,i} \times C_T \times C_L$$
(1)

where, F_i (ng/(m²·h)) is the estimated Hg emission flux for a given landuse type or a vegetation species i , $F_{s,i}$ (ng/(m²·h)) is the implemented emission factor for species i (Table 1), C_T is the temperature correction factor, and C_L is the solar radiation correction factor. In the evaluation of C_T and C_L , a equation analogous to Guenther Algorithm (Guenther *et al.*, 1995) for biogenic VOC emission was assumed because the emission-temperature-radiation relationship has not been yet available for Hg emission

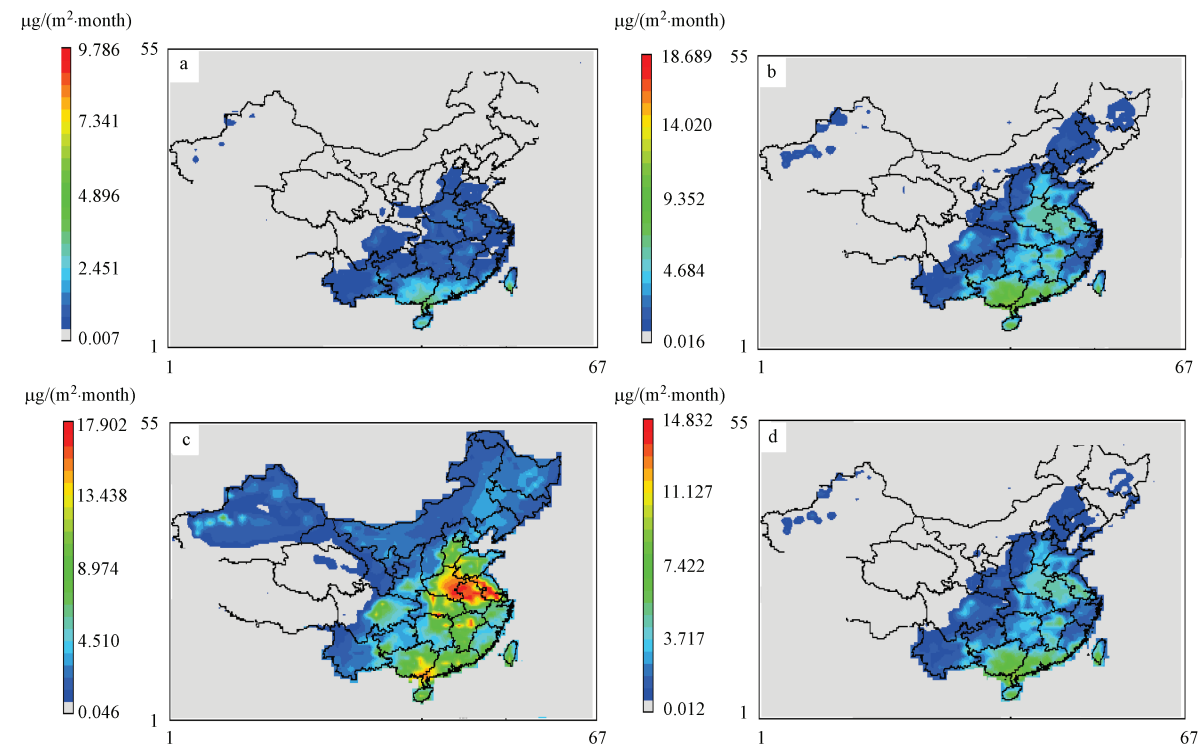


Fig. 1 Spatial distribution of the modeled vegetative mercury emissions at different season. (a) January; (b) April; (c) July; (d) October.

Table 1 Average daytime Hg emission intensities used in model runs (unit: ng/(m²·h))

	Case 1	Case 2	Reference
Urban	7.7*	31.0	Fang and Wang, 2004 (Case 2)
Irrigated agriculture	4.0	21.5	Lin <i>et al.</i> , 2005 (Case 1); Hou <i>et al.</i> , 2005b (Case 2)
Water	1.0	5.9	Pirrone <i>et al.</i> , 2001 (Case 1); Feng <i>et al.</i> , 2004 (Case 2)
Wetlands	40.0	40.0	Lindberg <i>et al.</i> , 2002
Forests	5.3	5.5	Hanson <i>et al.</i> , 1995 (Case 1); Fang and Wang, 2004 (Case 2)
Other plants	4.0	4.0	Lin <i>et al.</i> , 2005

* Estimated as 1/4 of Case 2.

from vegetation. This method has also been applied in the estimation of Hg emission in U.S. (Lin *et al.*, 2005).

Because of the uncertainty associated with the reported vegetative Hg fluxes, the model with two different sets of $F_{s,i}$ (Table 1) was used. In Case 1, the emission factors of the vegetation species except for urban are based on the work of Lin *et al.* (2005) who used the emission factors for estimating Hg emissions in the United States. Compared with the United States, the anthropogenic Hg emissions, the air concentration of Hg, and Hg deposition are much high in China, especially in urban and suburban areas or heavily polluted hotspots (Liu *et al.*, 2002; Feng *et al.*, 2002, 2003; Tan *et al.*, 2000), which would increase vegetative emissions correspondingly. Thus, Case 1 would only represent the lower limit of the vegetative emissions in China. In Case 2, the emission factors of the vegetation species are based on the observation in China. Some researchers assumed that the irrigated agriculture, water, and urban areas in China have emission flux intensities of 21.5 ng/(m²·h) (Hou *et al.*, 2005b), 5.92 ng/(m²·h) (Feng *et al.*, 2004), and 31 ng/(m²·h) (Fang and Wang, 2004), respectively. However, the above emission factor for agricultural fields was based on the limited observations which are only confined to suburb where soil Hg content is much higher than environmental background value (Hou *et al.*, 2005b; Zhang *et al.*, 2005). As aforementioned, high concentration of Hg in soil would lead to higher Hg emission, and vegetative emissions estimated in Case 2 would represent the upper limit in China. The emission factor for agricultural fields, in this article, is from observation at Ganzhuang (Hou *et al.*, 2005b), which is located in suburb of Guiyang City, with soil Hg content at 0.146 µg/g, amounting to approximately 2 times of environmental background value. But, lower than soil environmental quality standards (GB15618-1995; 0.15 µg/g) (Xia, 1996). Therefore, it is reasonable to take its emission factor (21.5 ng/(m²·h)) as the upper limit factor of the vegetative emission for agriculture in China.

Because Hg emission flux was measured only for a limited number of vegetation species, all the deciduous forest, evergreen forest, and mixed forest were grouped in the BELD3 data categories, and used the same average daytime emission as $F_{s,i}$ (5.5 ng/(m²·h)) for the tree vegetation groups (Table 1). Emission factor of dry crop, mixture zone of crop, grass and/or forest is assumed as 1/4 of irrigated crop in Case 2. The output from the model is temporally (hourly) and spatially resolved gridded emissions in network common data form format. The data in the subsequent maps are expressed as the emission intensity in each 81-km grid of the model domain.

2 Results and discussion

2.1 Spatial and temporal distribution of modeled emissions

Figure 1 shows the variation of modeled Hg emissions in January, April, July, and October. The results were obtained from the sum of hourly emission of each month

using the emission factor in Case 2 of Table 1. The distribution of Hg emission varies with seasons according to the change of surface temperature and solar intensity (Fig.1). The Hg emission could reach up to 18 µg/(m²·month) in July, whereas in January it was usually lower than 4 µg/(m²·month). In July, the vegetative emissions are mainly from the eastern and southern China due to the high temperature, large coverage area of agricultural landcover, and dense municipal groups.

The monthly Hg emissions for the two sensitivity cases are shown in Fig.2. As observed, the annual vegetative emissions are dominated by the emissions in June and August. In fact, approximately 50% of the annual emissions are generated during the three summer months, and approximately 80% of the annual vegetative emissions are generated from April to September. Summing up the monthly emissions for the entire year, the annual vegetative emissions for the two sensitivity cases are 79×10^3 kg (Case 1) and 177×10^3 kg (Case 2) (Table 2). Modeled Hg emissions in Case 2 are approximately 2 times of Case 1. This is caused mainly by the different agricultural emission factors between Case 1 and Case 2.

2.2 Comparison with anthropogenic Hg emissions

Vegetative Hg emissions release primarily as gaseous elemental mercury (GEM), whereas anthropogenic emissions release as GEM, reactive divalent mercury, and particulate mercury depending on the sources, fuel types, and emission control devices. Vegetative emissions, 79×10^3 kg (Case 1) and 177×10^3 kg (Case 2) (Table 2), account for 13% (Case 1) and 25% (Case 2) of the total Hg emissions and 21% (Case 1) and 37% (Case 2) of the total GEM emissions. Vegetative Hg emissions

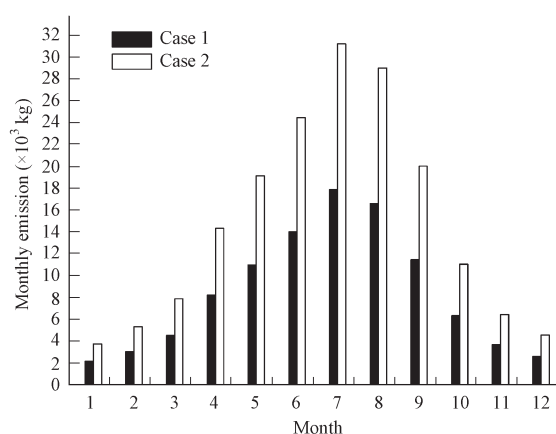


Fig. 2 Seasonal variation of the modeled vegetative mercury emissions in China domain for two sensitivity cases.

Table 2 Comparison of Hg emission and speciation by anthropogenic and vegetative sources in China (unit: $\times 10^3$ kg)

Hg	Anthropogenic ^a	Case 1	Case 2
Gaseous elemental mercury	300	79	177
Reactive divalent mercury	172	0	0
Particulate mercury	64	0	0
Total Hg	536	79	177

^a Data are obtained from Streets *et al.* (2005).

take up high percentage among total Hg emissions during summer. For example in July, vegetative emissions would account for 42% (Case 1) and 56% (Case 2) of the total GEM emissions. However, during winter, anthropogenic sources dominate the Hg emissions from vegetation due to the smaller emission caused by the much lower surface temperature and solar radiation. From the sensitivity analysis, it is concluded that Hg emissions from vegetation could constitute a significant fraction of the total mercury input to the atmosphere, and should be included in the emission inventory processing of Hg, especially during warm months.

Most mercury emission inventories only include anthropogenic emissions and neglect the large contribution of the natural mercury cycle because of difficulty in spatially estimating natural emissions and uncertainties in the natural emission process. Natural mercury emission was highlighted gradually with the research of the cycling of atmospheric mercury. Lin *et al.* (2005), Bash *et al.* (2004), and Pirrone *et al.* (2001) estimated natural mercury emission in the United States, Canada, and the Mediterranean region, respectively. In the work of Bash *et al.* (2004), the estimation of natural mercury flux were presented for only two weeks period during July. In the work of Pirrone *et al.* (2001), natural sources only include the volatilisation of elemental mercury from surface water and emissions from volcanoes, whereas the contribution from soil and vegetation was not included. Therefore, only the estimation by the authors is compared with that of Lin *et al.* (2005), who estimated the natural mercury emission in the continental United States to be 44×10^3 kg/year. In the present estimation, vegetative Hg emission in China was $(79\text{--}177) \times 10^3$ kg/year, which was approximately 2–4 times of that in the United States. It is commonly accepted among the mercury research community that mercury emission from vegetation is caused by the deposition of mobilized mercury by human activities, followed by the uptake and transpiration of elemental gaseous mercury by vegetation (Bishop *et al.*, 1998; Lindberg *et al.*, 2002, Obrist *et al.*, 2005). Anthropogenic mercury emission in China is estimated to be $536 (\pm 236) \times 10^3$ kg (Streets *et al.*, 2005), which is much higher than that in the United States (142×10^3 kg; Lin *et al.*, 2005). Therefore, high anthropogenic mercury emission might be the main reason that causes the difference of natural mercury emission between China and the United States.

2.3 Uncertainties in the simulation

Uncertainties associated with the current estimation are composed mainly of two parts. (1) Limited laboratory and field data have impeded the understanding of Hg emissions. Very few observations are carried out in China on Hg emission flux from vegetations and mainly confined to limited vegetation categories, so much landuse/vegetation categories were only assumed with the same emission factor in this article. Additional emission factors can be implemented in the model once further mercury flux data become available. (2) The Hg concentration in soil is also one key factor controlling Hg emission rate from soil to

the air, but soil/water mercury content on Hg exchange between vegetations and the atmosphere is not included in the model, which would cause a certain error in the simulation. To avoid the above uncertainties, 2 sets of emission factors to calculate the natural mercury emissions in China are selected, one is from the observation at relative clean regions (Lin *et al.*, 2005), the other is from the observation at light polluted regions of China. The range of natural mercury emission estimated in this work can represent the actual emission in China reasonably.

3 Conclusions

In this study, the vegetative mercury emissions in the BEIS3 framework in a 81-km model domain covering the Chinese continent was estimated. From the sensitivity analysis, it is estimated that the vegetative mercury emissions range from a lower limit of 79×10^3 kg/year to an upper limit of 177×10^3 kg/year. The vegetative emissions are mainly generated from the southern and eastern China, and exhibit strong diurnal and seasonal variations. The annual vegetative emissions are dominated by the emissions during June and August. In fact, approximately 50% of the annual emissions are generated during the three summer months, and approximately 80% of the annual vegetative emissions are generated from April to September. Vegetative emissions in China would account for 13% to 25% of the total Hg emissions, and 21% to 37% of the total GEM emissions.

Acknowledgments

This work was supported by the KIST-CAS Project, the Chinese Academy of Sciences (No. KZCX3-SW-443), and the National Nature Science Founding of China (No. 40473055).

References

- Bash J O, Miller D R, Meyer T H, Bresnahan P A, 2004. North-east United States and Southeast Canada natural mercury emissions estimated with a surface emission model. *Atmos Environ*, 38: 5683–5692
- Bishop K, Ying H, Munthe J, Dambrine E, 1998. Xylem sap as a pathway for total mercury and methyl mercury transport from soils to tree canopy in boreal forest. *Biogeochemistry*, 40: 101–113.
- Byun D, Ching J, 1999. Science algorithms of the EPA Models-3 Community Multiscale Air Quality (CMAQ) modeling system. Rep EPA-600/R-99/030. Office of Research and Development, US Environmental Protection Agency, Washington, DC.
- Carpi A, Lindberg S, 1998. Application of a teflon dynamic flux chamber for quantifying soil mercury flux: Tests and results over background soil. *Atmos Environ*, 32(5): 873–882.
- Fang F M, Wang Q C, Li Z B, 2001. Atmospheric particulate mercury concentration and its dry deposition flux in Changchun City, China. *Sci Total Environ*, 281: 229–236.
- Fang F M, Wang Q C, 2004. Mercury concentration, emission flux in urban land surface and its factors. *Environmental Chemistry*, 23(1): 109–110.

- Feng X B, Sommar J, Lindqvist O, Hong Y T, 2002. Occurrence, emissions and deposition of mercury during coal combustion in the province Guizhou. *Water Air Soil Pollut*, 139: 311–324.
- Feng X B, Tang S F, Shang L, Yan H, Sommar J, Lindqvist O, 2003. Total gaseous mercury in the atmosphere of Guiyang, China. *Sci Total Environ*, 304: 61–72.
- Feng X B, Yan H, Wang S L, Qiu G L, Tang S L, Shang L *et al.*, 2004. Seasonal variation of gaseous mercury exchange rate between air and water surface over Baihua reservoir, Guizhou, China. *Atmos Environ*, 38: 4721–4732.
- Feng X B, Wang S F, Qiu G L, Hou Y M, Tang S L, 2005. Total gaseous mercury emissions from soil in Guiyang, Guizhou, China. *J Geophys Res*, 110: D14306.
- Grell G, Dudhia J, Stauffer D, 1994. A description of the fifth generation Penn State/NCAR mesoscale model (MM5), NCAR Technical Note. NCAR TN-398STR, 138–142.
- Guenther A, Hewitt C, Erickson D, Fall R, Geron C, Graedel T *et al.*, 1995. A global model of natural volatile organic compound emissions. *J Geophys Res*, 100: 8873–8892.
- Gustin M, Lindberg S, Marsik F, Ebinghaus R, Edwards G, Fitzgerald C *et al.*, 1999. The Nevada STORMS mercury flux methods intercomparison. *J Geophys Res*, 104: 21831–21844.
- Gustin M, Coolbaugh M, Engle M, Fitzgerald B, 2003. Atmospheric mercury emissions from mine wastes and surrounding geologically enriched terrains. *Environ Geol*, 43: 339–351.
- Hanson P, Lindberg S, Tabberer T, Owens J G, Kim K H, 1995. Foliar exchange of mercury vapor: Evidence for a compensation point. *Water Air Soil Pollut*, 80: 373–382.
- Hou M, Qian J P, Yin H A, 2005a. A study on mercury species in Guilin soil. *Journal of Soil and Water Conservation*, 36(3): 398–401.
- Hou Y B, Feng X B, Wang S F, Qiu G L, 2005b. Mercury flux at air/soil interface in Guiyang and its suburbs. *Acta Pedologica Sinica*, 42(1): 52–58.
- Kim K, Hanson P, Barnett M, Lindberg S, 1997. Biogeochemistry of mercury in the air-soil-plant system. *Metal Ions in Biological Systems*, 34: 185–212.
- Lai Q H, Du H Y, Zhang Z J, Fang J W, Xia B, 2005. Formation of the high mercury in soil in the Pearl River Delta. *Environmental Chemistry*, 24(2): 219–220.
- Lamb B, Gay D, Westberg H, 1993. A biogenic hydrocarbon emission inventory for the USA using a simple forest canopy model. *Atmos Environ*, 27A: 1673–1690.
- Lin C J, Lindberg S, Ho T, Jang C, 2005. Development of a processor in BEIS3 for estimating vegetative mercury emission in the continental United States. *Atmos Environ*, 39: 7529–7540.
- Lin J P, Lai Q H, Fang J W, Ma S W, 2007. Appraise of environmental geochemistry in soil Hg polluted areas in the Pearl River Delta. *Ecology and Environment*, 16(1): 41–46.
- Lindberg S, 1996. Forest and the global biogeochemical cycle of mercury: the importance of understanding air/vegetation exchange process. In: *Regional and Global Mercury Cycles* (Baeyens W., ed.). NATO Advanced Science Institute Series, Dordrecht: Kluwer Academic Publishers. 359–380.
- Lindberg S, Dong W, Meyers T, 2002. Transpiration of gaseous elemental mercury through vegetation in a subtropical wetland in Florida. *Atmos Environ*, 36: 5207–5219.
- Liu S, Nadim F, Perkins C, Carley R J, Hoag G E, Lin Y *et al.*, 2002. Atmospheric mercury monitoring survey in Beijing, China. *Chemosphere*, 48: 97–107.
- Obrist D, Gustin M S, Arnone J A, Johnson D W, Schorr D E, Verburg P *et al.*, 2005. Measurements of gaseous elemental mercury fluxes over intact tall grass prairie monoliths during one full year. *Atmos Environ*, 39: 957–965.
- Pacyna J, Pacyna E, 2002. Global emissions of mercury from anthropogenic sources in 1995. *Water Air Soil Pollut*, 137: 149–165.
- Pirrone N, Costa P, Pacyna J, Ferrara R, 2001. Mercury emission to the atmosphere from natural and anthropogenic sources in the Mediterranean region. *Atmos Environ*, 35: 2997–3006.
- Rasmussen P, 1994. Current methods of estimating atmospheric mercury fluxes in remote areas. *Environ Sci Technol*, 28: 2233–2241.
- Streets D, Hao J M, Wu Y, Jiang J K, Chan M, Tian H Z *et al.*, 2005. Anthropogenic mercury emissions in China. *Atmos Environ*, 39: 7789–7806.
- Tan H, He J L, Liang L, Lazoff S, Sommer J, Xiao Z F *et al.*, 2000. Atmospheric mercury deposition in Guizhou, China. *Sci Total Environ*, 259: 223–230.
- Wang W T, Ma Z D, Zhao B, Gong M, 2005. The concentration and distribution characteristics of mercury in Gedian area, Wuhan. *Environment Chemistry*, 24(4): 454–458.
- Xia J, 1996. Detailed Explanation Soil Environmental Quality Standards. Beijing: China Environment Press, 84–86.
- Xiao Z F, Sommar J, Lindqvist O, Tan H, He J L, 1998. Atmospheric mercury deposition on Fanjing Mountain Nature Reserve, Guizhou, China. *Chemosphere*, 36(10): 2191–2200.
- Zhang H, Lindberg S, 1999. Processes influencing the emission of mercury from soils: a conceptual model. *J Geophys Res*, 104: 21889–21896.
- Zhang C, He L, Wang D Y, Zhang J Y, 2005. Soil/air interface mercury exchange fluxes of several ground surface in Chongqing. *Acta Scientiae Circumstantiae*, 25(8): 1085–1090.